Steel and Composite Structures, *Vol. 34, No. 4 (2020) 511-524*
DOI: https://doi.org/10.12989/scs.2020.34.4.511

A four variable trigonometric integral plate theory for hygro-thermo-mechanical bending analysis of AFG ceramic-metal plates resting on a two-parameter elastic foundation

Abdelouahed Tounsi*[1,2], S.U. Al-Dulaijan[1], Mohammed A. Al-Osta[1], Abdelbaki Chikh[2,3], M.M. Al-Zahrani[1], Alfarabi Sharif [1] and Abdeldjebbar Tounsi[2]

[1]*Department of Civil and Environmental Engineering, King Fahd University of Petroleum & Minerals, 31261 Dhahran, Eastern Province, Saudi Arabia*
[2]*Material and Hydrology Laboratory, University of Sidi Bel Abbes, Faculty of Technology, Civil Engineering Department, Algeria*
[3]*Université Ibn Khaldoun, BP 78 Zaaroura, 14000 Tiaret, Algérie*

(*Received August 4, 2019, Revised December 15, 2019, Accepted December 26, 2019*)

Abstract. In this research, a simple four-variable trigonometric integral shear deformation model is proposed for the static behavior of advanced functionally graded (AFG) ceramic-metal plates supported by a two-parameter elastic foundation and subjected to a nonlinear hygro-thermo-mechanical load. The elastic properties, including both the thermal expansion and moisture coefficients of the plate, are also supposed to be varied within thickness direction by following a power law distribution in terms of volume fractions of the components of the material. The interest of the current theory is seen in its kinematics that use only four independent unknowns, while first-order plate theory and other higher-order plate theories require at least five unknowns. The *"in-plane displacement field"* of the proposed theory utilizes cosine functions in terms of thickness coordinates to calculate out-of-plane shear deformations. The vertical displacement includes flexural and shear components. The elastic foundation is introduced in mathematical modeling as a two-parameter Winkler-Pasternak foundation. The virtual displacement principle is applied to obtain the basic equations and a Navier solution technique is used to determine an analytical solution. The numerical results predicted by the proposed formulation are compared with results already published in the literature to demonstrate the accuracy and efficiency of the proposed theory. The influences of *"moisture concentration"*, temperature, stiffness of foundation, shear deformation, geometric ratios and volume fraction variation on the mechanical behavior of AFG plates are examined and discussed in detail.

Keywords: advanced functionally graded materials; four-variable integral plate theory; hygro-thermo-mechanical loading; elastic foundation

1. Introduction

Advanced functionally graded material (AFGM) is a mixture of ceramic and metal with a targeted change in the volume fractions of two materials between the two faces of any structure. Unlike fibrous composite laminated plates, these are often affected by delamination and stress concentration influences. As a result, advanced functionally graded materials (AFGMs) are widely employed in many *"engineering structures"* that are subject to a severe thermal environment because of their attractive characteristics. Vel and Batra (2002), Chen *et al*. (2003) and Alibeigloo (2010) conducted three-dimensional (3D) investigations of *"functionally graded plates"* in a thermal environment. However, solutions of 3D equations are very difficult when a power law is considered for the gradation of the properties of materials. Therefore, various researchers have developed several two-dimensional *"approximate shear deformation theories"* to predict the bending behavior of mechanically or hygro-thermally loaded functionally graded plates. The conventional plate theory (CPT) established by *"Kirchhoff"* in 1850 for the bending of thin structures subjected to mechanical or *"hygro-thermal"* loading neglects the influence of *"transverse shear deformation"*. Therefore, it cannot be employed for thick plate in which the effects of shear deformation are greater. Chi and Chung (2006ab) presented CPT-based works to obtain a mathematical solution for functionally and *"exponentially graded plates"*. Using the classical beam theory, Civalek and Öztürk (2010) analyzed the free vibration of tapered beam-column with pinned ends embedded in Winkler-Pasternak elastic foundation. Eltaher *et al*. (2018) employed a classical beam theory and a modified porosity model for analyzing of FG porous nanobeams. Mindlin (1951) developed a new theory called *"first-order shear deformation theory"* (FSDT) which considers the influence of shear deformation. In this model, the transverse shear/strain repartition is supposed to be constant across the structure thickness and therefore a shear coefficient is needed (Nguyen *et al.* 2008, Benferhat *et al.* 2016, Avcar 2016, Avcar and Mohammed 2018, Avcar 2019). The shortcomings of CPT and FSDT led to the

*Corresponding author, Ph.D.
E-mail: tou_abdel@yahoo.com

ISSN: 1229-9367 (Print), 1598-6233 (Online)

development of *"higher order shear deformation theories"* (HSDTs) in order to overcome the use of shear correction coefficients and to ensure the traction free boundary conditions at the upper and lower faces of the structure. The *"third-order shear deformation theory"* is one of those HSDTs used by Reddy (2000) for FG plate analysis. An analytical solution for the bending of FG plates was obtained by Zenkour (2006) by applying the well known*"sinusoidal shear deformation theory"*. Gulshan Taj et al. (2013) proposed a *"finite element model"*taking into account seven degrees of freedom for each node for the bending analysis of rectangular and asymmetric FG plates based on the theory of third order shear deformation. Aliaga and Reddy (2004) developed a *"finite element model"* based on the theory of third order shear deformation to investigate the linear and nonlinear thermo-mechanical behavior of FG plates. Yaghoobi *et al.* (2014) presented an analytical study on post-buckling and the nonlinear dynamic response of FG beams resting on a nonlinear elastic foundation and subjected to thermo-mechanical loadings. Zidi *et al.* (2014) presented the flexural analysis of FGM plates resting on an elastic base and subjected to hygro-thermo-mechanical loading by employing a four-variable *"trigonometric shear deformation theory"*. Kar and Panda (2015) exploited the free vibration behavior of temperature-dependent FG curved panels under a thermal environment. Daouadji et al. (2016) discussed the bending behaviour of an imperfect FGM plates under hygro-thermo-mechanical loading with analytical validation. Sayyad and Ghugal (2017a) have developed a unified theory of shear deformation for the static analysis of FG plates and beams. Sayyad and Ghugal (2015, 2017b) have reviewed various refined and advanced models of beams and plates available in the scientific literature. Fazzolari (2016) also employed hierarchical refined plate theories to study the modal properties of FG plates composed of temperature-dependent materials and subjected to a *"temperature gradient"*. Chavan and Lal (2017) studied the dynamic bending response of SWCNT reinforced composite plates subjected to hygro-thermo-mechanical loading. Bouderba (2018) conducted a study on the bending of FGM rectangular plates resting on non-uniform elastic foundations in thermal environment using an accurate theory. Recently, Sayyad and Ghugal (2019) studied the effects of nonlinear hygro-thermo-mechanical loading on the bending of FG rectangular plates resting on an elastic foundation using a four-unknown plate theory. Other HSDTs can be found in the literature review where are used to study several mechanical behaviors of structures (Mahapatra and Panda 2015, Mahapatra *et al.* 2016a, Sharma *et al*. 2018 and 2019, Salah *et al.* 2019). In addition, it should be noted that in general, two types of methodologies are adopted for the analysis of hygrothermal modelling as is found in the literature (Mahapatra *et al.* 2016bc).

In this research, a simple four-variable trigonometric integral shear deformation theory containing undetermined integral terms in the kinematic, is proposed for the bending behavior of simply supported advanced functionally graded (AFG) ceramic-metal plates under non-linear hygro-thermo-mechanical loading and resting on an elastic foundation. The *"in-plane displacement field"* uses undetermined integral terms with cosine functions in terms of the z-coordinate to calculate out-of-plane shear deformations. The theory verifies tensile boundary conditions on the upper and lower faces of the structure without the use of problem-dependent shear correction coefficients. The material properties of the structure are assumed to be varied in the z-direction by following a simple power law distribution in terms of volume fractions of the constituents of the material. The virtual displacement principle is used to derive the basic equations. The foundation is introduced in a mathematical formulation as a two-parameter model *"Winkler–Pasternak foundation"*. A simply supported AFG ceramic-metal plate under a nonlinear hygro-thermo-mechanical load across the thickness is considered and the Navier solution is used for the *"detailed numerical study"*. The numerical results computed by the proposed theory are compared to theories available in the literature to demonstrate its efficiency and accuracy. The influences of *"moisture concentration"*, temperature, stiffness of foundation, shear deformation, geometric ratios and volume fraction variation on the mechanical behavior of AFG plates are examined and discussed in detail.

2. A simple four-variable trigonometric integral plate theory

In this article, the kinematics uses trigonometric functions in z coordinates to take into account the shear strains out of the plane. Unlike the conventional HSDTs and FSDT, the current theory has a simple displacement field that considers undetermined integral terms and only four variables

$$u(x,y,z,t)=u_0(x,y,t)-z\frac{\partial w_0}{\partial x}+k_1\, f(z)\int\theta(x,y,t)\,dx \quad (1a)$$

$$v(x,y,z)=v_0(x,y,t)-z\frac{\partial w_0}{\partial y}+k_2\, f(z)\int\theta(x,y,t)\,dy \quad (1b)$$

$$w(x,y,z,t)=w_0(x,y,t) \quad (1c)$$

here, u_0, v_0, w_0 *and* θ ,are the displacement functions of the median surface of the plate. The constants k_1 and k_2 depend on the plate's geometry. In this work, the shear strain shape function is given by

$$f(z)=\frac{z\left[\pi+2\cos\left(\pi z/h\right)\right]}{2+\pi}$$

The linear strain expressions derived from the kinematics of equations (1), are as follows

$$\begin{Bmatrix}\varepsilon_x\\ \varepsilon_y\\ \varepsilon_{xy}\end{Bmatrix}=\begin{Bmatrix}\varepsilon_x^0\\ \varepsilon_y^0\\ \varepsilon_{xy}^0\end{Bmatrix}+z\begin{Bmatrix}\varepsilon_x^1\\ \varepsilon_y^1\\ \varepsilon_{xy}^1\end{Bmatrix}+f(z)\begin{Bmatrix}\varepsilon_x^2\\ \varepsilon_y^2\\ \varepsilon_{xy}^2\end{Bmatrix},\ \begin{Bmatrix}\gamma_{xz}\\ \gamma_{yz}\end{Bmatrix}=g(z)\begin{Bmatrix}\gamma_{xz}^0\\ \gamma_{yz}^0\end{Bmatrix} \quad (2)$$

with

$$\left\{\begin{matrix}\varepsilon_x^0\\ \varepsilon_y^0\\ \varepsilon_{xy}^0\end{matrix}\right\}=\left\{\begin{matrix}\dfrac{\partial u_0}{\partial x}\\ \dfrac{\partial v_0}{\partial y}\\ \dfrac{\partial u_0}{\partial y}+\dfrac{\partial v_0}{\partial x}\end{matrix}\right\},\ \left\{\begin{matrix}\varepsilon_x^1\\ \varepsilon_y^1\\ \varepsilon_{xy}^1\end{matrix}\right\}=\left\{\begin{matrix}-\dfrac{\partial^2 w_0}{\partial x^2}\\ -\dfrac{\partial^2 w_0}{\partial y^2}\\ -2\dfrac{\partial^2 w_0}{\partial x\partial y}\end{matrix}\right\},$$

$$\left\{\begin{matrix}\varepsilon_x^2\\ \varepsilon_y^2\\ \varepsilon_{xy}^2\end{matrix}\right\}=\left\{\begin{matrix}k_1A'\theta\\ k_2B'\theta\\ k_1A'\dfrac{\partial}{\partial y}\int\theta dx+k_2B'\dfrac{\partial}{\partial x}\int\theta dy\end{matrix}\right\},\quad (4a)$$

$$\left\{\begin{matrix}\gamma_{xz}^0\\ \gamma_{yz}^0\end{matrix}\right\}=\left\{\begin{matrix}k_1A'\int\theta dx\\ k_2B'\int\theta dy\end{matrix}\right\}$$

and

$$g(z)=\frac{df(z)}{dz} \quad (4b)$$

By using the Navier type method, the integrals considered in the above equations can be treated via the following expressed:

$$\frac{\partial}{\partial y}\int\theta\,dx=A'\frac{\partial^2\theta}{\partial x\partial y},\ \frac{\partial}{\partial x}\int\theta\,dy=B'\frac{\partial^2\theta}{\partial x\partial y},$$
$$\int\theta\,dx=A'\frac{\partial\theta}{\partial x},\ \int\theta\,dy=B'\frac{\partial\theta}{\partial y} \quad (5)$$

where coefficients A', B', k_1 *and* k_2 are given by

$$A'=-\frac{1}{\mu^2},\ B'=-\frac{1}{\lambda^2},\ k_1=\lambda^2,\ k_2=\mu^2 \quad (6)$$

with λ and μ are defined in Eq. (16).

2.1 Material properties of AFG plate and constitutive equations:

The material characteristics of the AFG plate, like *"Young's modulus"* E, *"shear modulus"* G, *"thermal expansion coefficient"* α and "moisture expansion coefficient" β, are expressed according to the volume fraction of the "constituent materials". According to the power-law variation, these mechanical properties are given by

$$E(z)=E_m+\left(E_c-E_m\right)\left(\frac{2z+h}{2h}\right)^p \quad (7a)$$

$$G(z)=G_m+\left(G_c-G_m\right)\left(\frac{2z+h}{2h}\right)^p \quad (7b)$$

$$\alpha(z)=\alpha_m+\left(\alpha_c-\alpha_m\right)\left(\frac{2z+h}{2h}\right)^p \quad (7c)$$

$$\beta(z)=\beta_m+\left(\beta_c-\beta_m\right)\left(\frac{2z+h}{2h}\right)^p \quad (7d)$$

where E_c, G_c, α_c and β_c are the corresponding mechanical properties of metal and E_m, G_m, α_m and β_m are the corresponding ones for metal. p is the gradient index and $p\geq 0$. The lower surface of the AFG plate is ceramic rich and the upper surface is metal rich.

The examined AFG plate is subjected to the "mechanical load" and variations in temperature and moisture concentration. Thus, the *"stress–strain relationship"* for the AFG plate is as follows

$$\left\{\begin{matrix}\sigma_x\\ \sigma_y\\ \tau_{xy}\\ \tau_{xz}\\ \tau_{yz}\end{matrix}\right\}=\left[\begin{matrix}C_{11}&C_{12}&0&0&0\\ C_{12}&C_{22}&0&0&0\\ 0&0&C_{66}&0&0\\ 0&0&0&C_{55}&0\\ 0&0&0&0&C_{44}\end{matrix}\right]\left\{\begin{matrix}\varepsilon_x-\alpha\Delta T-\beta\Delta C\\ \varepsilon_y-\alpha\Delta T-\beta\Delta C\\ \gamma_{xy}\\ \gamma_{xz}\\ \gamma_{yz}\end{matrix}\right\} \quad (8)$$

where (σ_x, σ_y, τ_{xy}, τ_{xz}, τ_{yz}) and (ε_x, ε_y, γ_{xy}, γ_{xz}, γ_{yz}) are the stress and strain components respectively; $\Delta T=T-T_0$ and $\Delta C=C-C_0$, where T_0 is the initial temperature and C_0 is the initial moisture concentration. The temperature and moisture field variations across the thickness are assumed to be

$$\Delta T(x,y,z)=T_1(x,y)+\frac{z}{h}T_2(x,y)+\frac{f(z)}{h}T_3(x,y) \quad (9a)$$

$$\Delta C(x,y,z)=C_1(x,y)+\frac{z}{h}C_2(x,y)+\frac{f(z)}{h}C_3(x,y) \quad (9b)$$

where T_1, T_2 and T_3 are thermal loads; and C_1, C_2 and C_3 are hygro loads. The stiffness coefficients C_{ij} are expressed as

$$C_{11}(z)=C_{22}(z)=\frac{E(z)}{1-\nu^2},\ C_{12}(z)=\frac{\nu E(z)}{1-\nu^2} \quad (10a)$$

$$C_{66}(z)=C_{55}(z)=C_{44}(z)=\frac{E(z)}{2(1+\nu)} \quad (10b)$$

2.2 Governing equations

The governing equations can be deduced by employing the principle of "*virtual displacements*", which is analytically given by

$$\int_{-h/2}^{h/2}\int_{\Omega}\left[\sigma_x\delta\,\varepsilon_x+\sigma_y\delta\,\varepsilon_y+\tau_{xy}\delta\,\gamma_{xy}+\tau_{xz}\delta\,\gamma_{xz}+\tau_{yz}\delta\,\gamma_{yz}\right]d\,\Omega\,d\,z \\ -\int_{\Omega}(q-f_e)\,\delta\,w\,d\,\Omega=0 \tag{11}$$

where Ω is the top surface, and q is the "*applied transverse load*". f_e is the density of the reaction force of foundation. For the "*Winkler-Pasternak foundation model*" f_e is given by

$$f_e=k_w w(x,y)-k_{p1}\frac{\partial^2 w(x,y)}{\partial x^2}-k_{p2}\frac{\partial^2 w(x,y)}{\partial y^2} \tag{12}$$

where k_w is the Winkler parameter and k_p is the shear parameter.

The governing equations are derived from Eq. (11) by integrating the displacement gradients by parts and setting the coefficients of δu_0, δv_0, δw_0 and $\delta\theta$ to zero separately

$$\begin{aligned}
&\delta\,u_0: \quad \frac{\partial N_x}{\partial x}+\frac{\partial N_{xy}}{\partial y}=0\\
&\delta\,v_0: \quad \frac{\partial N_{xy}}{\partial x}+\frac{\partial N_y}{\partial y}=0\\
&\delta\,w_0: \quad \frac{\partial^2 M_x^b}{\partial x^2}+\frac{\partial^2 M_y^b}{\partial y^2}+2\frac{\partial^2 M_{xy}^b}{\partial x\partial y}+q-f_e=0\\
&\delta\,\theta: k_1\,A^{'}M_x^s+k_2\,B^{'}M_y^s+\left(k_1\,(A^{'})^2+k_2(B^{'})^2\right)\frac{\partial^2 M_{xy}^s}{\partial x\partial y}\\
&\qquad -k_1\,(A^{'})^2\frac{\partial Q_{xz}}{\partial x}-k_2(B^{'})^2\frac{\partial Q_{yz}}{\partial y}=0
\end{aligned} \tag{13}$$

where (N_x, N_y, N_{xy}) denote the total in-plane force resultants, (M_x^b, M_y^b, M_{xy}^b), (M_x^s, M_y^s, M_{xy}^s) are the total moment resultants and (Q_{xz}, Q_{yz}) are the transverse shear stress resultants and they are expressed as

$$\left(N_x,N_y,N_{xy}\right)=\int_{-h/2}^{h/2}\left(\sigma_x,\sigma_y,\tau_{xy}\right)dz \tag{14a}$$

$$\left(M_x^b,M_y^b,M_{xy}^b\right)=\int_{-h/2}^{h/2}\left(\sigma_x,\sigma_y,\tau_{xy}\right)zdz \tag{14b}$$

$$\left(M_x^s,M_y^s,M_{xy}^s\right)=\int_{-h/2}^{h/2}\left(\sigma_x,\sigma_y,\tau_{xy}\right)f(z)dz \tag{14c}$$

$$\left(Q_{xz},Q_{yz}\right)=\int_{-h/2}^{h/2}\left(\tau_{xz},\tau_{yz}\right)g(z)dz \tag{14d}$$

2.3. Analytical solution

In the current work, the Navier solution method is utilized to obtain an analytical solution for simply supported AFG rectangular plates. The unknowns variables are expressed as

$$\begin{Bmatrix}u_0\\v_0\\w_0\\\theta\end{Bmatrix}=\begin{Bmatrix}U_0\cos(\lambda\,x)\sin(\mu\,y)\\V_0\sin(\lambda\,x)\cos(\mu\,y)\\W_0\sin(\lambda\,x)\sin(\mu\,y)\\\theta_0\sin(\lambda\,x)\sin(\mu\,y)\end{Bmatrix} \tag{15}$$

where U_0, V_0, W_0 and θ_0 are arbitrary parameters to be determined, with

$$\lambda=\pi/a,\ \mu=\pi/b \tag{16}$$

The following trigonometric form is supposed for the hygro-thermo-mechanical loads (q, T_1, T_2, T_3, C_1, C_2, C_3)

$$\begin{Bmatrix}q\\T_1\\T_2\\T_3\\C_1\\C_2\\C_3\end{Bmatrix}=\begin{Bmatrix}q_0\sin(\lambda\,x)\sin(\mu\,y)\\t_1\sin(\lambda\,x)\sin(\mu\,y)\\t_2\sin(\lambda\,x)\sin(\mu\,y)\\t_3\sin(\lambda\,x)\sin(\mu\,y)\\c_1\sin(\lambda\,x)\sin(\mu\,y)\\c_2\sin(\lambda\,x)\sin(\mu\,y)\\c_3\sin(\lambda\,x)\sin(\mu\,y)\end{Bmatrix} \tag{17}$$

where q_0, t_1, t_2, t_3, c_1, c_2 and c_3 are the "*Fourier coefficients*" of hygro-thermo-mechanical loads.

Substitution of Eqs. (15) and (17) into the governing Eqs. (13) leads to the following system of algebraic equations

$$[C]\{\Delta\}=\{F\} \tag{18}$$

where $\{\Delta\}=\{U_0,V_0,W_0,\theta_0\}^t$ and $[C]$ is the symmetric matrix given by

$$[C]=\begin{bmatrix}S_{11}&S_{12}&S_{13}&S_{14}\\S_{12}&S_{22}&S_{23}&S_{24}\\S_{13}&S_{23}&S_{33}&S_{34}\\S_{14}&S_{24}&S_{34}&S_{44}\end{bmatrix} \tag{19}$$

in which the elements of stiffness matrix $[C]$ are as follows

$$\begin{aligned}
&S_{11}=\lambda^2A_{11}+\mu^2A_{66},\ S_{12}=\lambda\mu\left(A_{12}+A_{66}\right),\\
&S_{13}=-\left(\lambda\mu^2\left(B_{12}+B_{66}\right)+\lambda^3B_{11}\right)\\
&S_{14}=\lambda\left(-k_1A^{'}\lambda^2D_{11}-k_2B^{'}D_{12}+\mu^2D_{66}\left(k_1(A^{'})^2+k_2(B^{'})^2\right)\right)\\
&S_{22}=\mu^2A_{22}+\lambda^2A_{66}\\
&S_{23}=-\left(\lambda^2\mu\left(B_{12}+2B_{66}\right)+\mu^3B_{22}\right)\\
&S_{24}=\lambda^2\mu\left(k_1(A^{'})^2+k_2(B^{'})^2\right)D_{66}-\mu\left(k_1A^{'}D_{12}+k_2B^{'}D_{22}\right)\\
&S_{33}=-2\lambda^2\mu^2\left(E_{12}+2E_{66}\right)-\lambda^2\left(k_{p1}+\lambda^2E_{11}\right)-\mu^2\left(k_{p2}+\mu^2E_{22}\right)-k_w\\
&S_{34}=2\lambda^2\mu^2\begin{pmatrix}\left(k_1(A^{'})^2+k_2(B^{'})^2\right)F_{66}-\lambda^2\left(k_1A^{'}F_{11}+k_2B^{'}F_{12}\right)\\-\mu^2\left(k_1A^{'}F_{12}+k_2B^{'}F_{22}\right)\end{pmatrix}\\
&S_{44}=-k_1A^{'}\left(k_1A^{'}G_{11}+k_2B^{'}G_{12}\right)-k_2B^{'}\left(k_1A^{'}G_{12}+k_2B^{'}G_{22}\right)\\
&\qquad-\lambda^2\mu^2G_{66}\left(k_1(A^{'})^2+k_2(B^{'})^2\right)^2-\lambda^2\left(k_1^2(A^{'})^3\right)A_{55}^s-\mu^2\left(k_2^2(B^{'})^3\right)A_{44}^s
\end{aligned} \tag{20}$$

and stiffness components A_{ij}, B_{ij},.., are given as

$$\left(A_{ij},B_{ij},D_{ij},E_{ij},F_{ij},G_{ij}\right)=\int_{-h/2}^{h/2}C_{ij}\left(1,z,f(z),z^2,zf(z),f(z)^2\right)dz,\quad (i,j)=(1,2,6) \tag{21a}$$

$$A_{ij}^{s}=\int_{-h/2}^{h/2}C_{ij}\,g(z)^2dz,\,(i,j)=(4,5) \tag{21b}$$

and $\{F\}=\{F_1,F_2,F_3,F_4\}^t$ is a generalized force vector given by

$$F_1=-\lambda\left(\left(A_1^Tt_1+\frac{B_1^T}{h}t_2+\frac{B_1^{Ts}}{h}t_3\right)+\left(A_1^cc_1+\frac{B_1^c}{h}c_2+\frac{B_1^{cs}}{h}c_3\right)\right);$$

$$F_2=-\mu\left(\left(A_2^Tt_1+\frac{B_2^T}{h}t_2+\frac{B_2^{Ts}}{h}t_3\right)+\left(A_2^cc_1+\frac{B_2^c}{h}c_2+\frac{B_2^{cs}}{h}c_3\right)\right)$$

$$F_3=-\left(\begin{array}{l}\left(\left(B_1^T\left(\lambda^2+\mu^2\right)\right)t_1+\dfrac{\left(D_1^T\left(\lambda^2+\mu^2\right)\right)}{h}t_2+\dfrac{\left(D_1^{Ts}\left(\lambda^2+\mu^2\right)\right)}{h}t_3\right)\\+\left(\left(B_1^c\left(\lambda^2+\mu^2\right)\right)c_1+\dfrac{\left(D_1^c\left(\lambda^2+\mu^2\right)\right)}{h}c_2+\dfrac{\left(D_1^{cs}\left(\lambda^2+\mu^2\right)\right)}{h}c_3\right)+q_0\end{array}\right) \tag{22}$$

$$F_4=-\left(\begin{array}{l}B_1^{Ts}\left(A'k_1+B'k_2\right)t_1+\dfrac{\left(\left(A'k_1+B'k_2\right)D_1^{Ts}\right)}{h}t_2+\dfrac{\left(\left(A'k_1+B'k_2\right)H_1^{Ts}\right)}{h}t_3\\+\left(\left(A'k_1+B'k_2\right)B_1^{cs}\right)c_1+\dfrac{\left(\left(A'k_1+B'k_2\right)D_1^{cs}\right)}{h}c_2+\dfrac{\left(\left(A'k_1+B'k_2\right)H_1^{cs}\right)}{h}c_3\end{array}\right)$$

with stiffness components are given as

$$\left(A_i^T,B_i^T,D_i^T,B_i^{Ts},D_i^{Ts},H_i^{Ts}\right)=\int_{-h/2}^{h/2}\alpha(z)C_{ij}\left(1,z,z^2,f(z),z\,f(z),f(z)?\right)dz \tag{23a}$$

$$\left(A_i^C,B_i^C,D_i^C,B_i^{Cs},D_i^{Cs},H_i^{Cs}\right)=\int_{-h/2}^{h/2}\beta(z)C_{ij}\left(1,z,z^2,f(z),z\,f(z),f(z)?\right)dz \tag{23b}$$

3. Numerical results

In this section, the influences of the temperature, moisture and foundation parameters on the deflection and stresses of simply supported AFG plates resting on Pasternak foundations are examined and discussed. The AFG rectangular structures resting on Pasternak foundations are considered to be fabricated from ceramic (Zirconia) and metal (Titanium) with the following mechanical material properties:

- Metal (Titanium, Ti-6Al-4V): $E_m=66.2$ GPa, $\nu=0.33$, $\alpha_m=10.3\times(10^{-6}/°C)$, $\beta_m=0.33$
- Ceramic (Zirconia, ZrO_2): $E_c=117$ GPa, $\nu=0.33$, $\alpha_c=7.11\times(10^{-6}/°C)$, $\beta_c=0$

The initial temperature and humidity concentration are considered as 25°C and 0%, respectively. Numerical results are employed in terms of non-dimensional quantities (stresses and deflection). The following non-dimensional quantities are utilized to define the computed results

$$\begin{array}{l}\bar{w}=\dfrac{100D}{q_0a^4}w\left(\dfrac{a}{2},\dfrac{b}{2},0\right),\ \bar{\sigma}_x=\dfrac{1}{100q_0}\sigma_x\left(\dfrac{a}{2},\dfrac{b}{2},\dfrac{h}{2}\right),\\ \bar{\tau}_{xy}=\dfrac{1}{10q_0}\tau_{xy}\left(0,0,-\dfrac{h}{3}\right),\ \bar{\tau}_{xz}=\dfrac{1}{10q_0}\tau_{xz}\left(0,\dfrac{b}{2},z\right),\\ K_w=\dfrac{a^4k_w}{D},\ K_{p1}=\dfrac{a^2k_{p1}}{D},\ K_{p2}=\dfrac{b^2k_{p2}}{D},\\ and\ D=\dfrac{E_ch^3}{12\left(1-\nu^2\right)}\end{array} \tag{24}$$

The non-dimensional quantities of deflections and different types of stresses are presented in Tables 1-4. Numerical values obtained using the present simple four-variable trigonometric integral shear deformation theory are compared with those predicted by theories of Zidi et al. (2014), Reddy (2000), Touratier (1991), Sayyad and Ghugal (2019), FSDT of Mindlin (1951), and classical plate theory (CPT).

Table 1 provides the non-dimensional deflection of the square AFG plate resting on "*elastic foundations*" and subjected to "*sinusoidal mechanical*" and hygro-thrmo-mechanical loadings for different values of the gradient index. From this example, it can be concluded that the "*Winkler foundation*" parameter provides a higher value of deflection compared to those predicted by considering the "*Pasternak foundation*" parameters. The important values of deflection are found when a structure is subjected to nonlinear hygro-thrmo-mechanical load whereas the weak values of deflection are found when a structure is subjected to only a mechanical load. It is also noted that deflection increases with increasing the gradient index because of the reduction in the rigidity of the plate and diminishes with increasing the geometric ratio (*a/h*) of the AFG plates.

The variations of deflection versus the geometric ratio *a/h* are demonstrated in Figs. 1-3. The results presented in these figures show the influences of the "*Winkler foundation*" and "*Pasternak foundation*" coefficients on the deflections when the structure is subjected to a pure "*mechanical load*", linear hygro-thermo-mechanical load, and a nonlinear hygro-thermo-mechanical load, respectively. It can be seen from these figures that the influences of the foundation coefficients on the non-dimensional deflection of the AFG plates are felt more in the thick plates. It is indicated in Figures 1 to 3 that the deflection of the plate is greater when it is subjected to a hygro-thermo-mechanical load with respect to a pure mechanical load. This is due to that the nonlinear hygro-thermo-mechanical load, which presents considerable influences on the extensional behavior of the plate as compared to the flexural behavior. It is also observed that the deflection is minimum for $p=0$ and is maximum for $p=\infty$ in all kinds of loadings.

Table 2 presents the influences of the gradient index (p) on the non-dimensional deflection and stresses of a AFG rectangular plate ($b=3a$) resting on a Pasternak elastic foundation($K_w=100$, $K_{p1}=100$, $K_{p2}=100$) and

Table 1 Influence of gradient index on the non-dimensional deflections of AFG square (b=a) plates resting on elastic foundation and subjected to hygro-thermo-mechanical loading

											a/h					
											5		10		20	
p	K_w	K_{p1}	K_{p2}	q_0	t_1	t_2	t_3	c_1	c_2	c_3	Present	Ref[(a)]	Present	Ref[(a)]	Present	Ref[(a)]
0	100	0	0	100	0	0	0	0	0	0	0.2405	0.2350	0.2136	0.2122	0.2066	0.2062
				100	0	10	0	0	100	0	1.8330	1.8390	0.6258	0.6251	0.3106	0.3107
				100	0	10	10	0	100	100	3.0253	3.4058	0.9354	0.9574	0.3887	0.3894
	0	100	100	100	0	0	0	0	0	0	0.0437	0.0434	0.0427	0.0426	0.0424	0.0424
				100	0	10	0	0	100	0	0.3329	0.3404	0.1251	0.1256	0.0638	0.0638
				100	0	10	10	0	100	100	0.5494	0.6305	0.1869	0.1924	0.0798	0.0800
	100	100	100	100	0	0	0	0	0	0	0.0418	0.0416	0.0409	0.0409	0.0407	0.0407
				100	0	10	0	0	100	0	0.3190	0.3262	0.1200	0.1208	0.0612	0.0612
				100	0	10	10	0	100	100	0.5265	0.6042	0.1793	0.1845	0.0765	0.0768
1	100	0	0	100	0	0	0	0	0	0	0.2923	0.2862	0.2623	0.2607	0.2544	0.2540
				100	0	10	0	0	100	0	2.0862	2.4129	0.7299	0.8115	0.3726	0.3936
				100	0	10	10	0	100	100	3.4318	4.2935	1.0817	1.2118	0.4616	0.4991
	0	100	100	100	0	0	0	0	0	0	0.0451	0.0450	0.0443	0.0443	0.0441	0.0441
				100	0	10	0	0	100	0	0.3221	0.3806	0.1234	0.1383	0.0646	0.0683
				100	0	10	10	0	100	100	0.5298	0.7053	0.1828	0.2133	0.0800	0.0866
	100	100	100	100	0	0	0	0	0	0	0.0432	0.0430	0.0425	0.0424	0.0422	0.0422
				100	0	10	0	0	100	0	0.3082	0.3630	0.1181	0.1320	0.0619	0.0654
				100	0	10	10	0	100	100	0.5070	0.6749	0.1751	0.2043	0.0766	0.0830
2	100	0	0	100	0	0	0	0	0	0	0.3075	0.3007	0.2750	0.2732	0.2664	0.2659
				100	0	10	0	0	100	0	2.1253	2.5118	0.7512	0.8483	0.3869	0.4118
				100	0	10	10	0	100	100	3.4853	4.6982	1.1086	1.3138	0.4774	0.5222
	0	100	100	100	0	0	0	0	0	0	0.0455	0.0453	0.0447	0.0446	0.0445	0.0444
				100	0	10	0	0	100	0	0.3143	0.3786	0.1221	0.1386	0.0646	0.0688
				100	0	10	10	0	100	100	0.5154	0.7083	0.1801	0.2147	0.0797	0.0872
	100	100	100	100	0	0	0	0	0	0	0.0435	0.0434	0.0428	0.0427	0.0426	0.0425
				100	0	10	0	0	100	0	0.3006	0.3623	0.1168	0.1327	0.0618	0.0659
				100	0	10	10	0	100	100	0.4930	0.6776	0.1724	0.2055	0.0763	0.0835
5	100	0	0	100	0	0	0	0	0	0	0.3075	0.3154	0.2750	0.2854	0.2664	0.2774
				100	0	10	0	0	100	0	2.1253	2.6252	0.7512	0.8892	0.3869	0.4308
				100	0	10	10	0	100	100	3.4853	4.9469	1.1086	1.3799	0.4774	0.5469
	0	100	100	100	0	0	0	0	0	0	0.0458	0.0456	0.0450	0.0449	0.0448	0.0447
				100	0	10	0	0	100	0	0.3079	0.3800	0.1212	0.1400	0.0646	0.0695
				100	0	10	10	0	100	100	0.5034	0.7161	0.1783	0.2173	0.0795	0.0882
	100	100	100	100	0	0	0	0	0	0	0.0438	0.0436	0.0431	0.0430	0.0429	0.0428
				100	0	10	0	0	100	0	0.2944	0.3634	0.1160	0.1340	0.0619	0.0665
				100	0	10	10	0	100	100	0.4813	0.6849	0.1706	0.2080	0.0761	0.0844
∞	100	0	0	100	0	0	0	0	0	0	0.2405	0.3519	0.2136	0.3224	0.2066	0.3146
				100	0	10	0	0	100	0	1.5500	2.9516	0.5526	1.0017	0.2921	0.4872
				100	0	10	10	0	100	100	2.5304	5.4908	0.8071	1.5485	0.3564	0.6173
	0	100	100	100	0	0	0	0	0	0	0.0437	0.0463	0.0427	0.0458	0.0424	0.0456
				100	0	10	0	0	100	0	0.2815	0.3888	0.1104	0.1422	0.0600	0.0706
				100	0	10	10	0	100	100	0.4596	0.7233	0.1613	0.2198	0.0731	0.0895
	100	100	100	100	0	0	0	0	0	0	0.0418	0.0443	0.0409	0.0437	0.0407	0.0436
				100	0	10	0	0	100	0	0.2697	0.3716	0.1059	0.1360	0.0575	0.0675
				100	0	10	10	0	100	100	0.4403	0.6913	0.1547	0.2102	0.0702	0.0856

[(a)] Taken from Sayyad and Ghugal (2019)

under a sinusoidal mechanical load. The computed results are in excellent agreement with those predicted by other theories showing that the present simple four-variable trigonometric integral shear deformation model is able to investigate the mechanical response of the AFG plate. It should be noted that, as the gradient index increases for the AFG plates, the deflection increases.

The inclusion of the basic Winkler parameter gives results of greater magnitude than those obtained with the inclusion of Pasternak's basic parameters. The reverse influence of the gradient index is observed on results of stresses of the AFG plate. Indeed, the computed stresses are reduced with increasing the gradient index.

Table 2 Influence of gradient index on non-dimensional deflections and stresses of AFG rectangular plates (b/a=3) resting on elastic foundation and under mechanical load (a/h=10, q_0 =100, t_1= t_2= t_3=0, c_1= c_2= c_3=0)

p	K_w	K_{p1}	K_{p2}	Theory	$\bar{w}$	$\bar{\sigma}_x$	$\bar{\tau}_{xy}$	$\bar{\tau}_{xz}$
0	100	100	100	Present	0.08226	0.04921	0.07008	0.04356
				Ref[a]	0.08227	0.04927	0.07068	0.03700
				Zidi *et al.* (2014)	0.08228	0.04919	0.06972	0.04116
				Reddy (2000)	0.08228	0.04919	0.06972	0.04116
				Touratier (1991)	0.08227	0.04919	0.06972	0.04246
				Mindlin (1951)	0.08228	0.04890	0.06986	0.03293
				CPT	0.08201	0.05035	0.07193	-
1	100	100	100	Present	0.08417	0.04575	0.05216	0.03403
				Ref[a]	0.08416	0.04580	0.05181	0.02924
				Zidi *et al.* (2014)	0.08418	0.04574	0.05190	0.03214
				Reddy (2000)	0.08417	0.04574	0.05190	0.03214
				Touratier (1991)	0.08418	0.04574	0.05191	0.03318
				Mindlin (1951)	0.08418	0.04546	0.05198	0.02572
				CPT	0.08399	0.04683	0.05353	-
2	100	100	100	Present	0.08456	0.04542	0.04794	0.03131
				Ref[a]	0.08453	0.04549	0.04776	0.02633
				Zidi *et al.* (2014)	0.08457	0.04539	0.04770	0.02951
				Reddy (2000)	0.08457	0.04539	0.04770	0.02951
				Touratier (1991)	0.08457	0.04540	0.04770	0.03050
				Mindlin (1951)	0.08457	0.04515	0.04781	0.02303
				CPT	0.08437	0.04655	0.04931	-
5	100	100	100	Present	0.08491	0.04655	0.04573	0.02910
				Ref[a]	0.08487	0.04665	0.04616	0.02450
				Zidi *et al.* (2014)	0.08491	0.04652	0.04549	0.02735
				Reddy (2000)	0.08491	0.04652	0.04549	0.02735
				Touratier (1991)	0.08492	0.04656	0.04549	0.02832
				Mindlin (1951)	0.08491	0.04630	0.04568	0.02085
				CPT	0.08471	0.04780	0.04714	-
Metal	100	100	100	Present	0.08583	0.02905	0.04137	0.02572
				Ref[a]	0.08582	0.02909	0.04174	0.02184
				Zidi *et al.* (2014)	0.08584	0.02905	0.04115	0.02428
				Reddy (2000)	0.08584	0.02905	0.04115	0.02428
				Touratier (1991)	0.08584	0.02906	0.04116	0.02507
				Mindlin (1951)	0.08584	0.02888	0.04126	0.01943
				CPT	0.08569	0.02978	0.04250	-

[a] Taken from Sayyad and Ghugal (2019)

The comparison of the numerical results (deflection and stresses) of AFG rectangular plates resting on Pasternak elastic foundation and under mechanical and linear hygro-thermal loading is presented in Table 3. When the numerical results of Tables 2 and 3 are compared, it should be noted that the deflection and the stresses are increased because of the inclusion of hygro-thermal influences. A very good agreement is demonstrated between the calculated results and those given by other researchers for all values of the gradient index.

The numerical results of the non-dimensional deflection and the stresses of AFG rectangular plates for nonlinear hygro-thermo-mechanical loading are reported in Table 4. It is observed that the deflections and stresses generated in the AFG plate in the case of the nonlinear hygro-thermo-mechanical load are more important in comparison with the case of pure mechanical and linear hygro-thermo-mechanical loadings. This is due to the expansion of the structure. The comparison carried out between the computed results and those given by other theories validates the efficiency of the proposed theory for predicting the bending behavior of an AFG plate resting on Pasternak foundation and subjected to nonlinear hygro-thermo-mechanical loading.

Fig. 4 presents the variation of the non-dimensional in-plane normal stress $\bar{\sigma}_x$ across the thickness of the AFG rectangular plates resting on an elastic foundation($K_w = 100$, $K_{p1} = 100$, $K_{p2} = 100$). It can be observed from this figure that the variation of $\bar{\sigma}_x$ is nonlinear for $p = 2$, 5, and 10. The nonlinearity influence becomes more important as the plate is subjected to the nonlinear hygro-thermo-mechanical

Table 3 Influence of gradient index on non-dimensional deflections and stresses of AFG rectangular plates(b/a=3) resting on elastic foundation and under linear hygro-thermo-mechanical load (a/h=10, q_0 =100, t_1= t_3=0, t_2=10, c_1= c_3=0, c_2=100)

p	K_w	K_{p1}	K_{p2}	Theory	$\bar{w}$	$\bar{\sigma}_x$	$\bar{\tau}_{xy}$	$\bar{\tau}_{xz}$
0	100	100	100	Present	0.17266	0.50297	0.17581	0.40819
				Ref[(a)]	0.17304	0.50437	0.17493	0.34779
				Zidi *et al.* (2014)	0.17309	0.50498	0.17490	0.38766
				Reddy (2000)	0.17309	0.50498	0.17490	0.38766
				Touratier (1991)	0.17309	0.50716	0.17495	0.40007
				Mindlin (1951)	0.17309	0.50245	0.17351	0.31024
1	100	100	100	Present	0.18457	0.51268	0.15698	0.46946
				Ref[(a)]	0.18500	0.51459	0.15668	0.40486
				Zidi *et al.* (2014)	0.18504	0.51450	0.15631	0.44545
				Reddy (2000)	0.18504	0.51450	0.15631	0.44545
				Touratier (1991)	0.18504	0.51476	0.15635	0.45984
				Mindlin (1951)	0.18505	0.51084	0.15494	0.35542
2	100	100	100	Present	0.18511	0.50165	0.13522	0.46362
				Ref[(a)]	0.18559	0.50394	0.13423	0.40012
				Zidi *et al.* (2014)	0.18560	0.50336	0.13451	0.43831
				Reddy (2000)	0.18560	0.50336	0.13451	0.43831
				Touratier (1991)	0.18560	0.50363	0.13461	0.45337
				Mindlin (1951)	0.18567	0.49980	0.13244	0.33958
5	100	100	100	Present	0.18646	0.48782	0.12494	0.46400
				Ref[(a)]	0.18699	0.49072	0.12515	0.39206
				Zidi *et al.* (2014)	0.18696	0.48940	0.12417	0.43754
				Reddy (2000)	0.18696	0.48940	0.12417	0.43754
				Touratier (1991)	0.18694	0.48967	0.12431	0.45322
				Mindlin (1951)	0.18712	0.48601	0.12125	0.32978
1	100	100	100	Present	0.18791	0.59246	0.12150	0.48443
				Ref[(a)]	0.18837	0.43102	0.12186	0.41102
				Zidi *et al.* (2014)	0.18840	0.43095	0.12087	0.45993
				Reddy (2000)	0.18840	0.43095	0.12087	0.45993
				Touratier (1991)	0.18840	0.43117	0.12092	0.47465
				Mindlin (1951)	0.18840	0.42794	0.11921	0.36808

[(a)] Taken from Sayyad and Ghugal (2019)

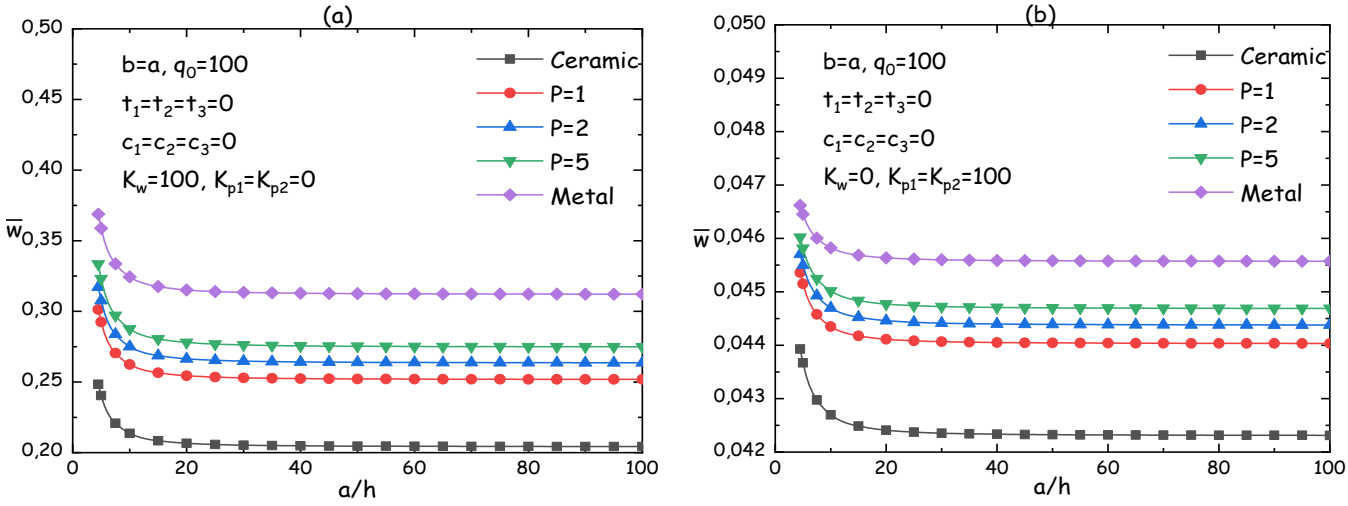

Continued-

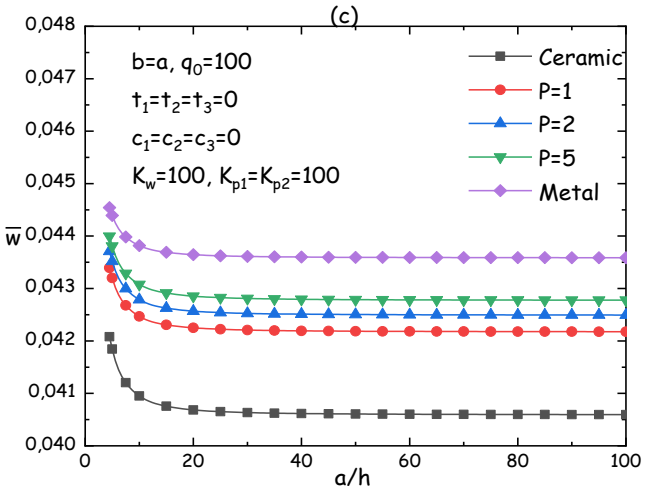

Fig. 1 Variation of non-dimensional transverse displacement ($\bar{w}$) with respect to aspect ratio (*a/h*) for square AFG plate resting on elastic foundations and subjected to mechanical load

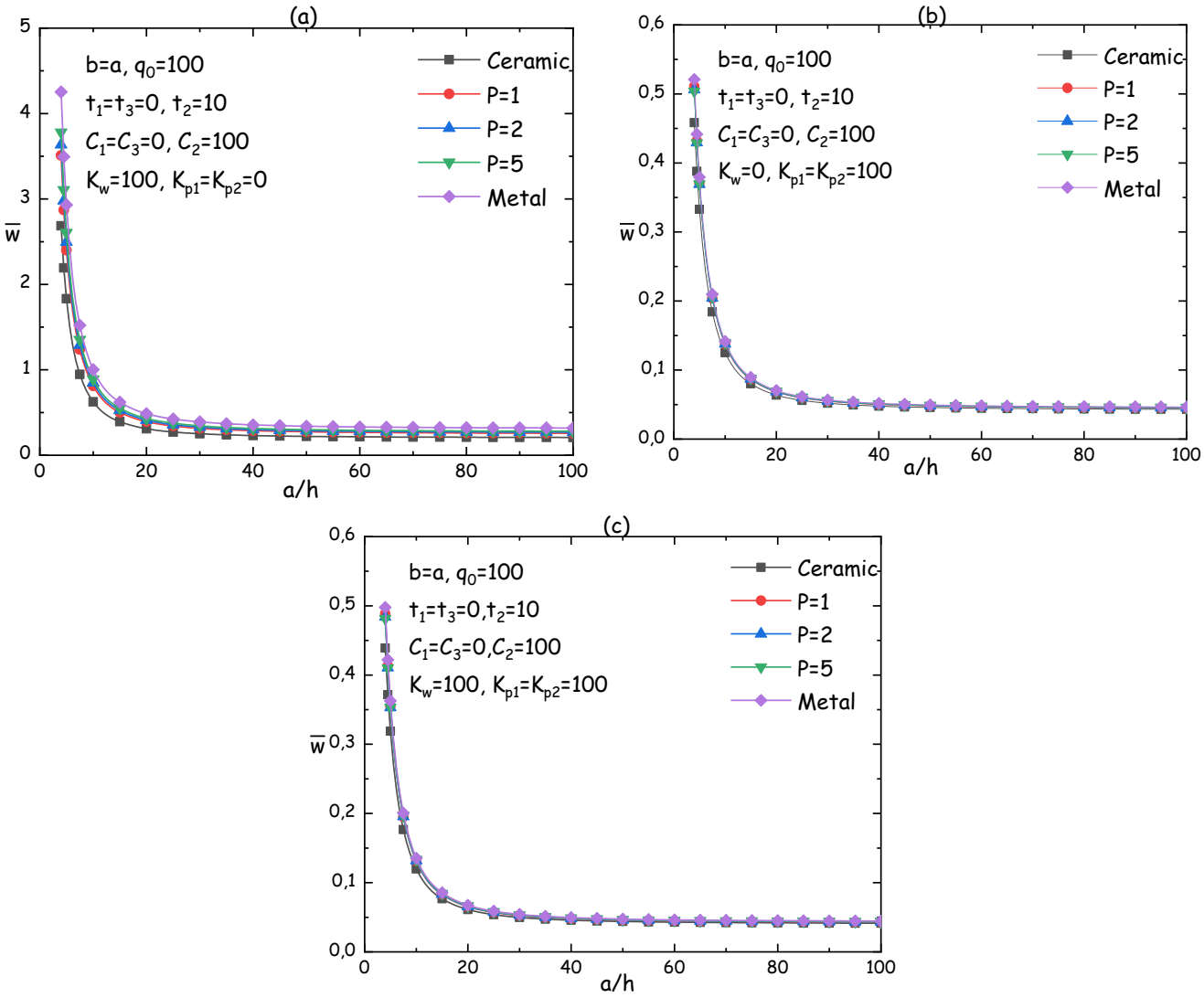

Fig. 2 Variation of non-dimensional transverse displacement ($\bar{w}$) with respect to aspect ratio (*a/h*) for square AFG plate resting on elastic foundations and subjected to linear hygro-thermo-mechanical load

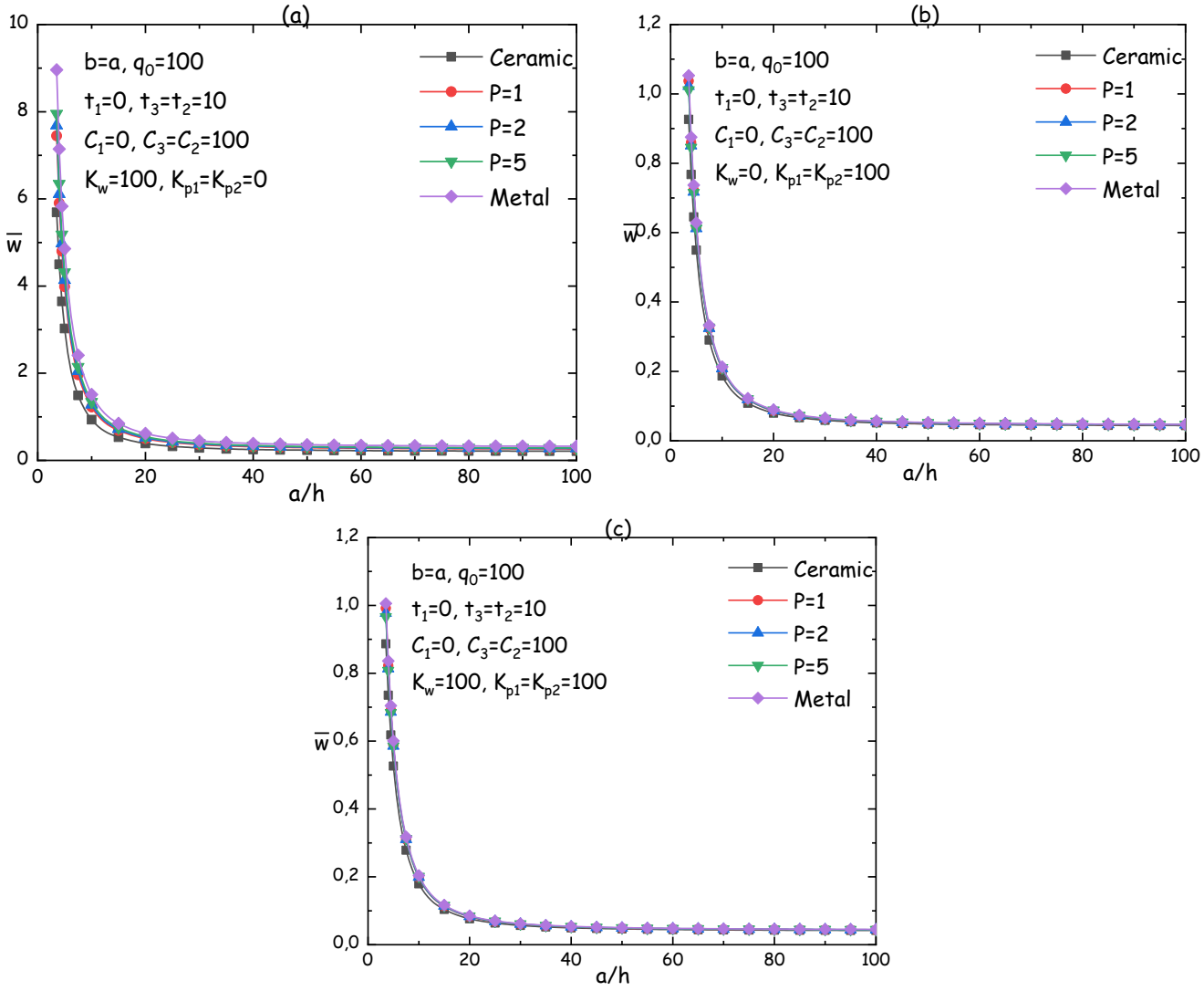

Fig. 3 Variation of non-dimensional transverse displacement ($\bar{w}$) with respect to aspect ratio (a/h) for square AFG plate resting on elastic foundations and subjected to nonlinear hygro-thermo-mechanical load

loads. It is also seen that the $\bar{\sigma}_x$ is in a compressive state at the upper face and a tensile state at the lower face. Figs. 5 and 6 present the influences of foundation coefficients and different loading conditions on the variations of $\bar{\tau}_{xy}$ and $\bar{\tau}_{xz}$ across the plate.

4. Conclusions

In this study, the hygro-thermo-mechanical bending behavior of advanced functionally graded rectangular plates based on the two-parameter elastic foundation is investigated using the theory of four-variable trigonometric shear deformation. The theory considers the tensile boundary conditions on the upper and lower surfaces of the plate without the need for "*shear correction factors*". The Navier solution is used to obtain the analytical solutions for simply supported "*boundary conditions*". The influences of foundation stiffness and gradient index on the hygro-thermo-mechanical behaviors of AFG plates are examined. The current four-variable model predicts excellent non-dimensional displacements and stresses over those predicted using five-variable plate models. The theory accounts for the nonlinear variation of temperature and humidity concentration over the entire thickness of the plate. Finally, this work will help us to design advanced functionally graded materials to ensure better durability and efficiency for hygro-thermal environments. An improvement of the present formulation will be considered in the future work to consider other type of materials (Kar *et al.* 2015, Mahapatra and Panda 2016, Mehar et al. 2017, Sahoo *et al.* 2016, 2017, Hirwani *et al.* 2018, Mehar and Panda 2018, Panjehpour *et al.* 2018, Shahadat *et al.* 2018, Faleh *et al.* 2018, Selmi and Bisharat 2018, Hussain and Naeem 2019, Fadoun 2019).

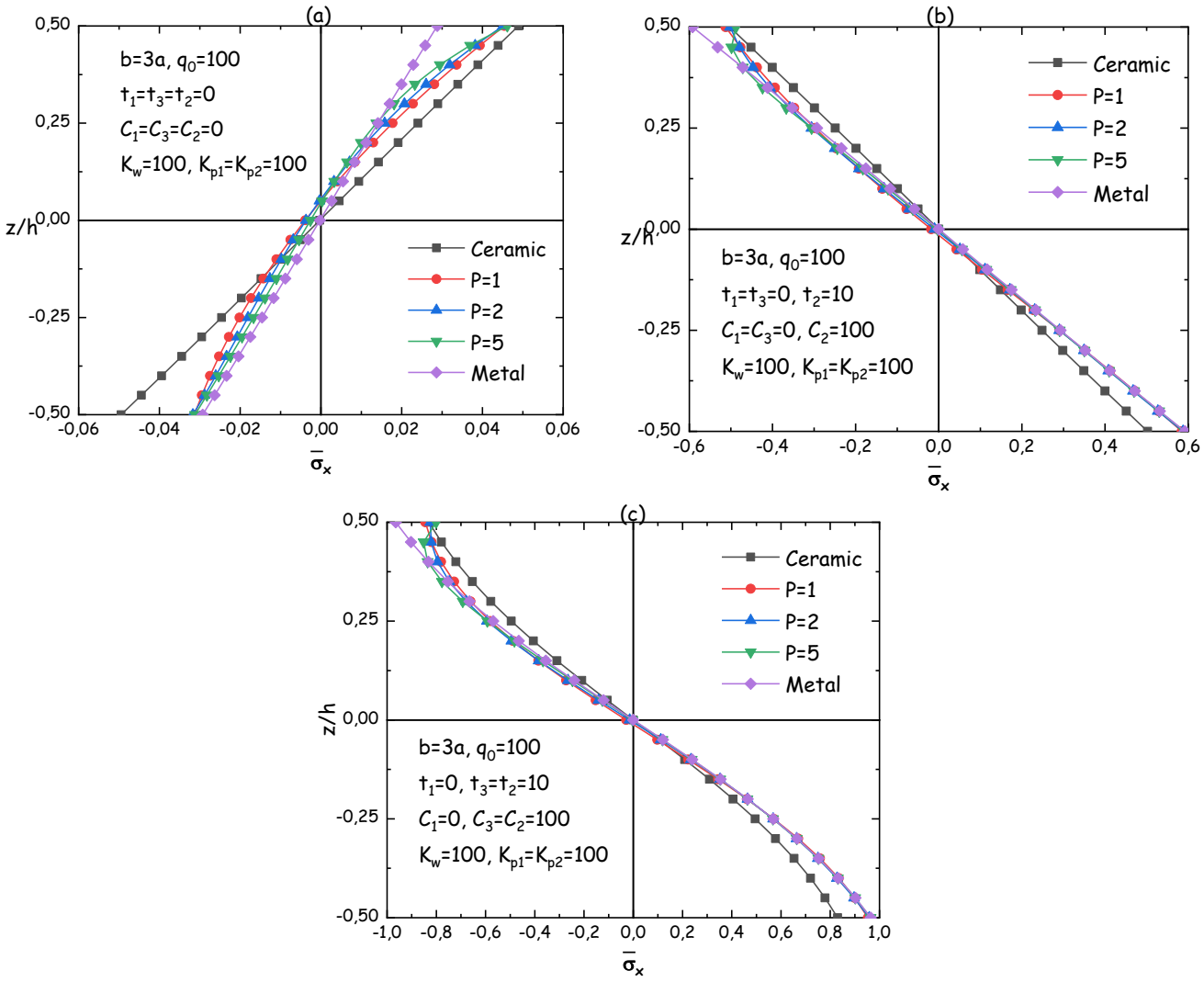

Fig. 4 Through thickness variation of non-dimensional in-plane normal stress ($\bar{\sigma}_x$) for rectangular AFG plate resting on elastic foundations

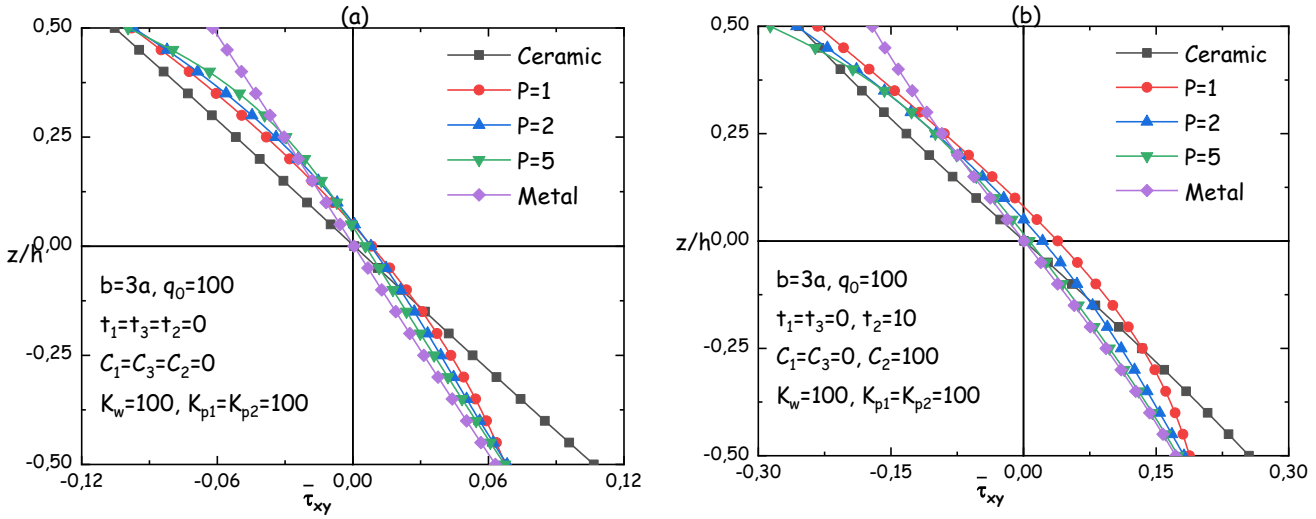

Continued-

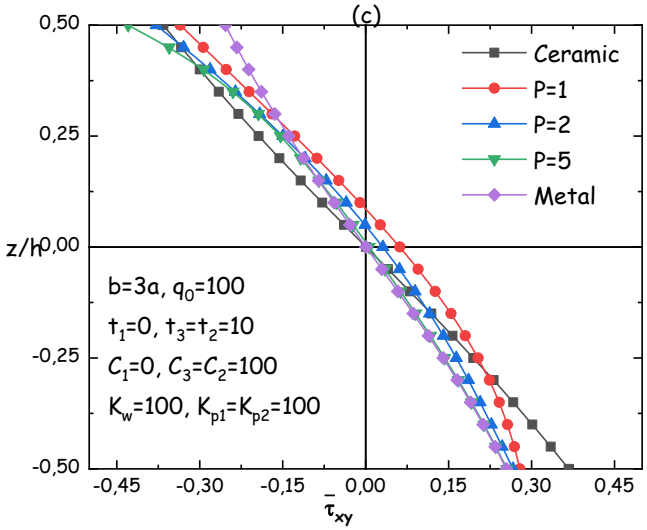

Fig. 5 Through thickness variation of non-dimensional in-plane shear stress ($\bar{\tau}_{xy}$) for rectangular AFG plate resting on elastic foundations

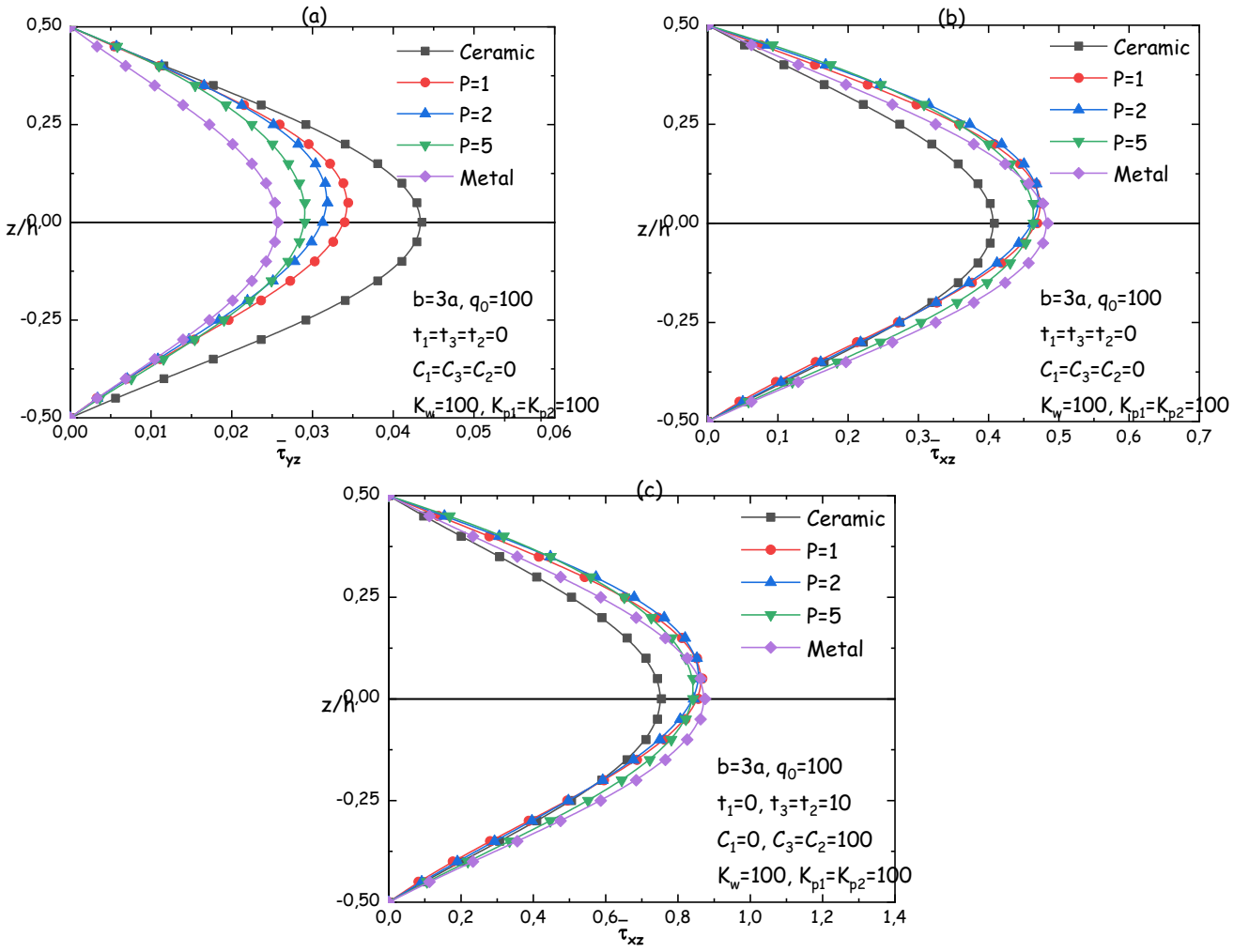

Fig. 6 Through thickness variation of non-dimensional transverse shear stress ($\bar{\tau}_{xz}$) for rectangular AFG plate resting on elastic foundations

Acknowledgments

The authors would like to acknowledge the support provided by the Deanship of Scientific Research (DSR) at King Fahd University of Petroleum & Minerals (KFUPM), Saudi Arabia for funding this work through Project No. DF181032. The support provided by the Department of Civil and Environmental Engineering is also acknowledged.

References

Aliaga, J.W. and Reddy, J.N. (2004), "Nonlinear thermoelastic analysis of functionally graded plates using the third-order shear deformation theory", *Int. J. Comp. Eng. Sci.*, **5**(4), 753-779. https://doi.org/10.1142/S146587630400266.

Alibeigloo, A. (2010), "Exact solution for thermo-elastic response of functionally graded rectangular plates", *Compos. Struct.*, **92**(1), 113-121. https://doi.org/10.1016/j.compstruct.2009.07.003.

Avcar, M. (2019), "Free vibration of imperfect sigmoid and power law functionally graded beams", *Steel Compos. Struct.*, **30**(6), 603-615. https://doi.org/10.12989/scs.2019.30.6.603.

Avcar, M. and Mohammed, W.K.M. (2018), "Free vibration of functionally graded beams resting on Winkler-Pasternak foundation", *Arabian J. Geosci.*, **11**(10), 232. https://doi.org/10.1007/s12517-018-3579-2.

Avcar, M. (2016), "Effects of material non-homogeneity and two parameter elastic foundation on fundamental frequency parameters of Timoshenko beams", *Acta Physica Polonica A*, **130**(1), 375-378. DOI: 10.12693/APhysPolA.130.375.

Benferhat, R., HassaineDaouadji, T., Hadji, L. and Said Mansour, M. (2016), "Static analysis of the FGM plate with porosities", *Steel Compos. Struct.*, **21**(1), 123 -136. https://doi.org/10.12989/scs.2016.21.1.123.

Bouderba, B. (2018), "Bending of FGM rectangular plates resting on non-uniform elastic foundations in thermal environment using an accurate theory", *Steel Compos. Struct.*, **27**(3), 311-325. https://doi.org/10.12989/scs.2018.27.3.311.

Chavan, S.G. and Lal, A. (2017), "Dynamic bending response of SWCNT reinforced composite plates subjected to hygro-thermo-mechanical loading", *Comput. Concrete*, **20**(2), 229-246. https://doi.org/10.12989/cac.2017.20.2.229.

Chen, W.Q., Bian, Z. and Ding, H. (2003), "Three-dimensional analysis of a thick FGM rectangular plate in thermal environment", *J. Zhejiang Univ. Sci.*, **4**(1), 1-7. https://doi.org/10.1007/BF02841071.

Chi, S.H. and Chung, Y.L. (2006a), "Mechanical behavior of functionally graded material plates under transverse load–Part I: analysis", *Int. J. Solids Struct.*, **43**(13), 3657-3674. https://doi.org/10.1016/j.ijsolstr.2005.04.011.

Chi, S.H. and Chung, Y.L. (2006b), "Mechanical behavior of functionally graded material plates under transverse load –Part II: numerical results", *Int. J. Solids Struct.*, **43**(13), 3675-3691. https://doi.org/10.1016/j.ijsolstr.2005.04.010

Civalek, Ö. and Öztürk, B. (2010), "Free vibration analysis of tapered beam-column with pinned ends embedded in Winkler-Pasternak elastic foundation", *Geomech. Eng.*, **2**(1), 45-56. https://doi.org/10.12989/gae.2010.2.1.045.

Daouadji, T.H., Adim, B. and Benferhat, R. (2016), "Bending analysis of an imperfect FGM plates under hygro-thermo-mechanical loading with analytical validation", *Adv. Mater. Res.*, **5**(1), 35-53. https://doi.org/10.12989/amr.2016.5.1.035.

Eltaher, M.A., Fouda, N., El-midany, T. and Sadoun, A.M. (2018), "Modified porosity model in analysis of functionally graded porous nanobeams", *J. Brazilian Soc. Mech. Sci. Eng.*, **40**, 141. https://doi.org/10.1007/s40430-018-1065-0.

Fadoun, O.O. (2019), "Analysis of axisymmetric fractional vibration of an isotropic thin disc in finite deformation", *Comput. Concrete*, **23**(5), 303-309. https://doi.org/10.12989/cac.2019.23.5.303.

Faleh, N.M., Ahmed, R.A. and Fenjan, R.M. (2018), "On vibrations of porous FG nanoshells", *Int. J. Eng. Sci.*, **133**, 1-14. ttps://doi.org/10.1016/j.ijengsci.2018.08.007.

Fazzolari, F.A. (2016), "Modal characteristics of P- and S-FGM plates with temperature-dependent materials in thermal environment", *J. Therm. Stresses*, **39**(7), 854-873. https://doi.org/10.1080/01495739.2016.1189772.

Gulshan Taj, M.N.A., Chakrabarti, A. and Sheikh, A.H. (2013), "Analysis of functionally graded plates using higher order shear deformation theory", *Appl. Math. Model.*, **37**(18-19), 8484-8494. https://doi.org/10.1016/j.apm.2013.03.058.

Hirwani, C.K., Biswash, S.,Mehar, K. and Panda, S.K. (2018), "Numerical flexural strength analysis of thermally stressed delaminated composite structure under sinusoidal loading", *IOP Conf. Series: Materials Science and Engineering*, **338**, 012019. doi:10.1088/1757-899X/338/1/012019

Hussain, M. and Naeem, M.N. (2019), "Rotating response on the vibrations of functionally graded zigzag and chiral single walled carbon nanotubes", *Appl. Math. Model.*, **75**, 506-520.

Kar, V.R. and Panda, S.K. (2015), "Free vibration responses of temperature dependent functionally graded curved panels under thermal environment", *Latin Am. J. Solids Struct.*, **12**, 2006-2024. http://dx.doi.org/10.1590/1679-78251691.

Kar, V.R., Mahapatra, T.R. and Panda, S.K. (2015), "Nonlinear flexural analysis of laminated composite flat panel under hygro-thermo-mechanical loading", *Steel Compos. Struct.*, **19**(4), 1011-1033. https://doi.org/10.12989/scs.2015.19.4.1011.

Mahapatra, T.R., Panda, S.K. and Dash, S. (2016a), "Effect of hygrothermal environment on the nonlinear free vibration responses of laminated composite plates: A nonlinear Unite element micromechanical approach", *IOP CONFERENCE SERIES: MATERIALS SCIENCE and Engineering*, **149**(1), 012151.

Mahapatra, T.R., Panda, S.K. and Kar, V.R. (2016b), "Nonlinear flexural analysis of laminated composite panel under hygro-thermo-mechanical loading — A Micromechanical Approach", *Int. J. Comput. Methods*, **13**(3), 1650015.

Mahapatra, T.R., Panda, S.K. and Kar, V.R. (2016c), "Geometrically nonlinear flexural analysis of hygro-thermo-elastic laminated composite doubly curved shell panel", *Int. J. Mech. Mater. Design*, **12**(2), 153-171.

Mahapatra, T.R., Panda, S.K. (2016), "Hygrothermal effects on the flexural strength of laminated composite cylindrical panels", *IOP Conference Series: Materials Science and Engineering*, **115**(1), 012040.

Mahapatra, T.R. and Panda, S.K. (2015), "Effects of hygrothermal conditions on free vibration behaviour of laminated composite structures", *IOP CONFERENCE SERIES: MATERIALS SCIENCE and Engineering*, **75**(1), 012016.

Mehar, K., Panda, S.K. and Patle, B.K. (2017), "Thermoelastic vibration and flexural behavior of FG-CNT reinforced composite curved panel", *Int. J. Appl. Mech.*, **9**(4), 1750046. https://doi.org/10.1142/S1758825117500466.

Mehar, K. and Panda, S.K. (2018), "Nonlinear finite element solutions of thermoelastic flexural strength and stress values of temperature dependent graded CNT-reinforced sandwich shallow shell structure", *Struct. Eng. Mech.*, **67**(6), 565-578. https://doi.org/10.12989/sem.2018.67.6.565.

Mindlin, R.D. (1951), "Influence of rotatory inertia and shear on flexural motions of isotropic elastic plates", *ASME J. Appl. Mech.*, **18**, 31-38.

Nguyen, T.K., Sab, K. and Bonnet, G. (2008), "First-order shear

deformation plate models for functionally graded materials", *Compos. Struct.*, **83**(1), 25-36. https://doi.org/10.1016/j.compstruct.2007.03.004.

Reddy, J.N. (2000), "Analysis of functionally graded plates", *Int. J. Numer. Meth. Eng.*, **47**(1-3), 663-684. https://doi.org/10.1002/(SICI)1097-0207(20000110/30)47:1/3<663::AID-NME787>3.0.CO;2-8.

Panjehpour, M., Woo, E., Loh, K. and Deepak, T.J. (2018), "Structural Insulated Panels: State-of-the-Art", *Trends in civil Engineering and its architecture*, **3**(1) 336-340.

Sahoo, S.S., Panda, S.K. and Singh, V.K. (2016), "Nonlinear flexural analysis of shallow carbon/epoxy laminated composite curved panels: experimental and numerical investigation", *J. Eng. Mech.*, **142**(4), 04016008. https://doi.org/10.1061/(ASCE)EM.1943-7889.0001040

Sahoo, S.S., Panda, S.K., Singh, V.K., Mahapatra, T.R. (2017), "Numerical investigation on the nonlinear flexural behaviour of wrapped glass/epoxy laminated composite panel and experimental validation", *Arch. Appl. Mech.*, **87**(2), 315-333. https://doi.org/10.1007/s00419-016-1195-8.

Sayyad, A.S. and Ghugal, Y.M. (2019), "Effects of nonlinear hygrothermomechanical loading on bending of FGM rectangular plates resting on two-parameter elastic foundation using four-unknown plate theory", *J. Therm. Stresses*, **42**(2), 213-232. https://doi.org/10.1080/01495739.2018.1469962.

Sayyad, A.S. and Ghugal, Y.M. (2017a), "A unified shear deformation theory for the bending of isotropic, functionally graded, laminated and sandwich beams and plates", *Int. J. Appl. Mech.*, **9**(1), 1-36. https://doi.org/10.1142/S1758825117500077.

Sayyad, A.S. and Ghugal, Y.M. (2017b), "Bending, buckling and free vibration of laminated composite and sandwich beams: a critical review of literature", *Compos. Struct.*, **171**, 486-504. s://doi.org/10.1016/j.compstruct.2017.03.053.

Sayyad, A.S. and Ghugal, Y.M. (2015), "On the free vibration analysis of laminated composite and sandwich plates: a review of recent literature with some numerical results", *Compos. Struct*., **129**, 177-201. https://doi.org/10.1016/j.compstruct.2015.04.007.

Selmi, A. and Bisharat, A. (2018), "Free vibration of functionally graded SWNT reinforced aluminum alloy beam", *J. Vibroeng*., **20**(5), 2151-2164. https://doi.org/10.21595/jve.2018.19445.

Shahadat, M.R.B., Alam, M.F., Mandal, M.N.A. and Ali, M.M. (2018), "Thermal transportation behaviour prediction of defective graphene sheet at various temperature: A Molecular Dynamics Study", *Am. J. Nanomater.*, **6**(1), 34-40.

Sharma, N., Mahapatra, T.R. and Panda, S.K. (2018), "Numerical analysis of acoustic radiation responses of shear deformable laminated composite shell panel in hygrothermal environment", *J. Sound Vib.*, **431**, 346-366. tps://doi.org/10.1016/j.jsv.2018.06.007.

Sharma, N., Mahapatra, T.R. and Panda, S.K. (2019), "Hygrothermal effect on vibroacoustic behaviour of higher-order sandwich panel structure with laminated composite face sheets", *Eng. Struct.*, **197**, 109355. https://doi.org/10.1016/j.engstruct.2019.109355.

Touratier, M. (1991), "An efficient standard plate theory", *Int. J. Eng. Sci.*, **29**(8), 901-916. https://doi.org/10.1016/0020-7225(91)90165-Y.

Vel, S., Batra, R. (2002), "Exact solution for thermoelastic deformations of functionally graded thick rectangular plates", *AIAA J.*, **40**(7), 1421-1433. https://doi.org/10.2514/2.1805.

Yaghoobi, H., Valipour, M.S., Fereidoon, A. and Khoshnevisrad, P. (2014), "Analytical study on post-buckling and nonlinear free vibration analysis of FG beams resting on nonlinear elastic foundation under thermo-mechanical loadings using VIM", *Steel Compos. Struct.*, **17**(5), 753-776. http://dx.doi.org/10.12989/scs.2014.17.5.753.

Zenkour, A.M. (2006), "Generalized shear deformation theory for bending analysis of functionally graded plates", *Appl. Math. Model.*, **30**(1), 67-84. ttps://doi.org/10.1016/j.apm.2005.03.009.

Zidi, M., Tounsi, A., Houari, M.S.A., Adda Bedia, E.A. and Beg, O.A. (2014), "Bending analysis of FGM plates under hygro-thermo-mechanical loading using a four variable refined plate theory", *Aerosp. Sci. Technol.*, **34**, 24-34. https://doi.org/10.1016/j.ast.2014.02.001.

CC